Langmuir–Blodgett Patterning: A Bottom–Up Way To Build Mesostructures over Large Areas

XIAODONG CHEN, STEVEN LENHERT,† MICHAEL HIRTZ, NAN LU,‡ HARALD FUCHS, AND LIFENG CHI*

Physikalisches Institut and Center for Nanotechnology (CeNTech), Westfälische Wilhelms-Universität, 48149 Münster, Germany

Received October 25, 2006

ABSTRACT

This Account describes a new paradigm, Langmuir–Blodgett (LB) patterning, for large-area patterning with mesostructured features based on the well-established LB technique. This strategy uses a simple fabrication technique to control the alignment, size, shape, and periodicity of self-organized phospholipid monolayer patterns with feature sizes down to 100 nm over surface areas of square centimeters. Because of the anisotropic wetting behavior of the patterns, they can be used as templates to direct the self-assembly of functional molecules and nanocrystals. Furthermore, the chemical patterns can be converted into topographical structures, which can be used to direct cell growth and organize nanocrystals. The mesoscopic structured surfaces described here may serve as a platform in engineering the biological/material interface and constructing biofunctionalized structures and "programmed" systems.

Introduction

The formation of patterned surfaces is a universal and fascinating phenomenon in nature, for example, regular stripes on the surface of zebras and the wings of butterflies.[1] Moreover, surface patterning has become an increasingly important part in modern science and technology, such as in the areas of micro-electronics, information processing and storage, nano/microfluidic devices, and biodetection.[2,3] Fabrication and investigation of patterned surfaces are active areas of research in chemistry, physics, materials science, and biology. Methods used for pattern fabrication are commonly summarized as "top–down" and "bottom–up". In the top–down approach, the features are written directly or transferred onto a substrate, e.g., by optical and e-beam lithography, and then the microscopic and/or nanoscopic features are engraved by applying appropriate etching and deposition processes. Although there is much focus on overcoming practical limits in fabricating small features,[4] another important limit is how large of an area can be efficiently patterned with small features. This limit arises because to write small features it is necessary to focus on a smaller surface area.[5] The concepts of self-assembly and self-organization provide an alternative way to realize small features over large areas via bottom–up approaches,[6] which rely on the interactions of building blocks, such as molecules or particles, which spontaneously assemble into nano/microstructures. The self-assembly and self-organization processes and the characteristics of the surface patterns (shape, size, function, etc.) can be controlled by tailoring the properties of building blocks.

The Langmuir–Blodgett (LB) technique is a well-established and sophisticated method to control interfacial molecular orientation and packing.[7,8] Moreover, it is an efficient approach toward the controllable fabrication of laterally patterned structures on solid supports, termed LB patterning. Laterally structured LB monolayers are normally generated by the deposition of ordered two-dimensional (2D) domains formed at the air–water interface onto solid substrates.[9–12] Alternatively, the LB transfer process itself can be used to form patterns near the three-phase contact line from a homogeneous Langmuir monolayer.

* To whom correspondence should be addressed. E-mail: chi@uni-muenster.de.

† Present address: Institut für NanoTechnologie, Forschungszentrum Karlsruhe GmbH, 76344 Eggenstein-Leopoldshafen, Germany.

‡ Present address: Key Laboratory for Supramolecular Structure and Materials of Ministry of Education, Jilin University, 130023 Changchun, People's Republic of China.

Xiaodong Chen received his B.S. degree (honors) in chemistry from Fuzhou University in 1999, M.S. degree (honors) in physical chemistry from the Chinese Academy of Sciences (Institute of Chemistry) under M. H. Liu in 2002, and Ph.D. degree (Summa Cum Laude) in biochemistry from the University of Muenster under H. Fuchs and L. F. Chi in 2006. He is currently a postdoctoral fellow working with C. A. Mirkin at Northwestern University. His research interests include self-assembly, nanotechnology, surface science, and biophysics.

Steven Lenhert received his B.S. degree in biochemistry from Messiah College (2000) and a Dr.rer.nat. in biology (University of Muenster, 2004). He is now a scientist at the Forschungszentrum Karlsruhe (2005–present). His current research is focused on dip-pen nanolithography of supported lipid membranes.

Michael Hirtz received his M.S. degree in physics from the University of Muenster in 2005. He is now working as a Ph.D. student in the field of self-organized surface patterning in the group of L. F. Chi and H. Fuchs.

Nan Lu received her B.S., M.S., and Ph.D. (2000) degrees in chemistry from Jilin University, China. She performed postdoctoral research with L. F. Chi and H. Fuchs in Germany and with G. Leggett in the U.K. from 2001 to 2004. She currently has a position as a professor at the Key Laboratory of Supramolecular Structure and Materials, Jilin University, China, since 2004. She is currently focused on LB patterning, self-assembly, and nanofabrication.

Harald Fuchs is Professor of experimental physics at the University of Muenster, Germany, and Scientific Director of the Center of Nanotechnology (CeNTech) in Muenster. His research focuses on nanoscale science and nanotechnology, ranging from scanning probe microscopy to self-organized nanostructure fabrication, and nano-bio systems. He has published more than 280 scientific articles in top journals. He was awarded the Philip Morris Research Prize "Challenge Future" in 1994 and the Münsterland Innovation Prize in 2001. He is currently a member of various scientific organizations including the German Science Academy "Leopoldina".

Lifeng Chi studied physics (B.S.) and physical chemistry (M.S.) at Jilin University. She received her Ph.D. degree at the Max Planck Institute for Biophysical Chemistry, Goettingen, Germany (1989). She received a Lisa Meitner scholarship in 1997. In 2000, she finished her habilitation working on nanostructuring through self-organization in thin organic films and became a professor in physics at the University of Muenster in 2004. Her research interests include surface nanopatterning by bottom–up strategies, scanning tunneling microscopy (STM)/AFM investigation on molecular assemblies, and the connection between micro- and nanostructures.

10.1021/ar600019r CCC: $37.00 © 2007 American Chemical Society
Published on Web 04/19/2007

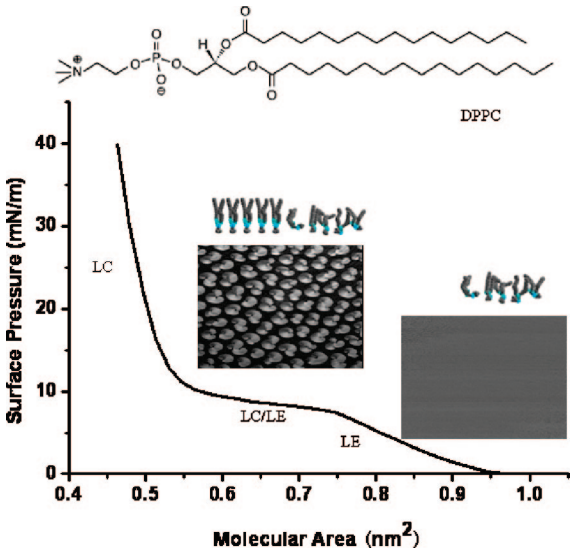

FIGURE 1. Phase behavior of the DPPC monolayer at the air–water interface. (Top) Chemical structure of DPPC. (Bottom) surface pressure–molecular area (π–*A*) isotherm of DPPC (~23 °C) and typical Brewster angle microscope (BAM) images (430 × 537 μm^2) for the liquid-expanded (LE) phases and LE/liquid-condensed (LC) phase transition along with the corresponding conformations of the DPPC molecules.

This Account sketches our recent works in fabrication of mesostructured patterns, which have lateral dimensions between the nano- and microscales, over larger areas by the LB technique. First, strategies to form mesostructures from a homogeneous L-α-dipalmitoylphosphatidylcholine (DPPC; chemical structure shown in Figure 1) Langmuir monolayer and to control the shape, size, and alignment of patterns are presented.[13–18] Second, the application of the patterns as templates to direct the self-assembly of molecules and nanocrystals is described.[19–24] Finally, pattern transfer procedures used for directing cell growth and nanocrystal patterning are discussed.[25–27]

Fabrication of Controllable Mesostructures

DPPC, one of the major lipid components of biological membranes, shows a typical phase behavior of a Langmuir monolayer at the air–water interface, characterized by a liquid-expanded (LE) phase, a liquid-condensed (LC) phase, and a LE–LC phase transition, confirmed by the surface pressure–molecular area (π–*A*) isotherm and Brewster angle microscope (BAM) images (Figure 1).[28,29] In the LE phase, the DPPC monolayer behaves as a quasi-2D liquid, where the head groups of the DPPC molecules are translationally disordered and chains are conformationally disordered. When the molecular areas are decreased, DPPC molecules begin to condense and a co-existing phase of LE and crystalline LC occurs at the plateau region of the isotherm. Finally, a homogeneous well-packed condensed monolayer (LC phase) appears at larger molecular areas.

Formation of Mesostructures with Nanochannels. Our fabrication approach uses the LB transfer process to induce phase transitions (i.e., substrate-mediated condensation) and create patterns near the three-phase contact line from a homogeneous DPPC Langmuir monolayer at the LE phase.[13,14] The resulting mesostructured DPPC, detected on surfaces by an atomic force microscope (AFM), consists of alternating stripes with widths of about 800 nm separated by channels of about 200 nm in width (Figure 2b).[14] Although it is difficult to directly observe the stripe formation *in situ* at the three-phase contact line in this system, one can imagine the process of stripe pattern formation as depicted in the schematic illustration of Figure 2a. The height difference between the stripes and channels is about 1 nm, and the stripes are composed of condensed (LC phase) DPPC molecules. Considering that the length of a DPPC molecule is about 2 nm, we can attribute the material in the channels to the expanded (similar to LE phase) DPPC molecules, which has a larger tilt angle compared to condensed DPPC molecules in the stripes, as depicted in Figure 2c. We confirmed this hypothesis with dynamic force spectroscopy measurements, where we can accurately detect the tip–sample interaction forces and distinguish the different phases (to be published).

Importantly, the size and shape of the DPPC patterns can be controlled by simply adjusting the transfer velocity, surface pressure, temperature, substrate chemistry, monolayer composition, and transfer method. This ability is essential to realizing applications in surface patterning.

Effect of Surface Pressure and Transfer Velocity. Firstly, the shape and lateral size of the DPPC stripe pattern from the pure DPPC monolayer strongly depends upon the transfer surface pressure and transfer velocity.[17,25] For instance, on mica substrates, at a surface pressure of 3.0 mN/m, a high transfer velocity of 60 mm/min induces the formation of horizontal DPPC stripes, parallel to the three-phase contact line (parts a and d of Figure 3). In contrast, vertical stripes, perpendicular to the three-phase contact line (parts c and f of Figure 3) are obtained at a low transfer velocity (10 mm/min). At a transfer velocity of 40 mm/min, a grid pattern, clearly showing the superposition of horizontal stripes and vertical stripes, is observed (Figure 3b). In general, the horizontal stripes only appear at the high transfer velocity (60 mm/min) with low transfer surface pressure, and the pure vertical stripes only appear at the low transfer velocity and high transfer surface pressure (still in LE phase).

Effect of the Substrate. Different hydrophilic substrates can be used to obtain DPPC mesostructures, but experimental conditions for the pattern formation are different because of the different surface properties. One reason for the stripe pattern formation is the substrate-mediated condensation of DPPC during the LB transfer; therefore, the molecule–substrate interaction should be a very important factor in this dynamic self-organization process. For instance, the periodic stripe patterns can be formed on an oxygen plasma-treated silicon surface, but the transfer velocity used has to be slower than that for transfer onto a mica surface at the same surface pressure and temperature.[20] Moreover, different treatment of the silicon substrate will affect the DPPC pattern formation (to be published). At the same transfer velocity, the surface

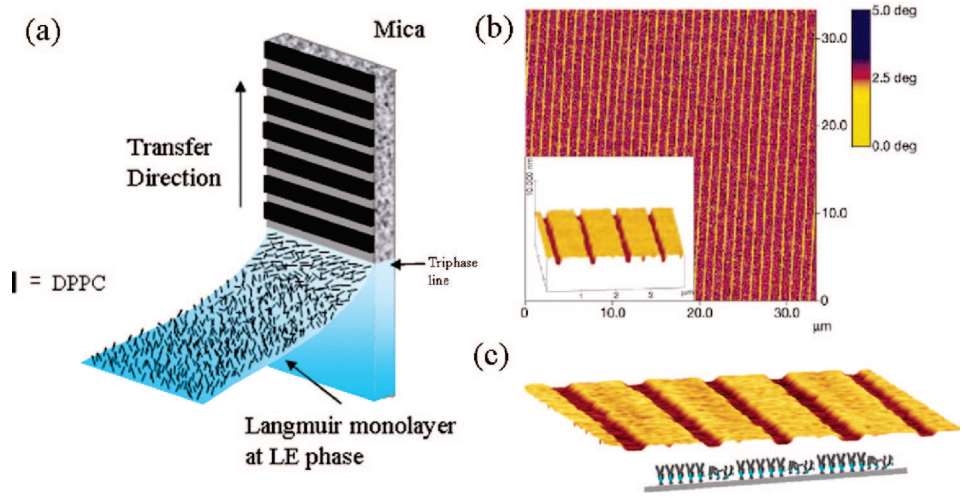

FIGURE 2. (a) Schematic illustration of the process of mesopattern formation. (b) Mesostructures with nanochannels on mica in phase (main figure) and topography (inset) imaging. Experimental conditions: surface pressure, 3 mN/m; transfer velocity, 60 mm/min; and temperature, 22.5 °C. (c) Composition of DPPC pattern: the DPPC stripe pattern is composed of expanded DPPC molecules in the channels and condensed DPPC molecules in the stripes.

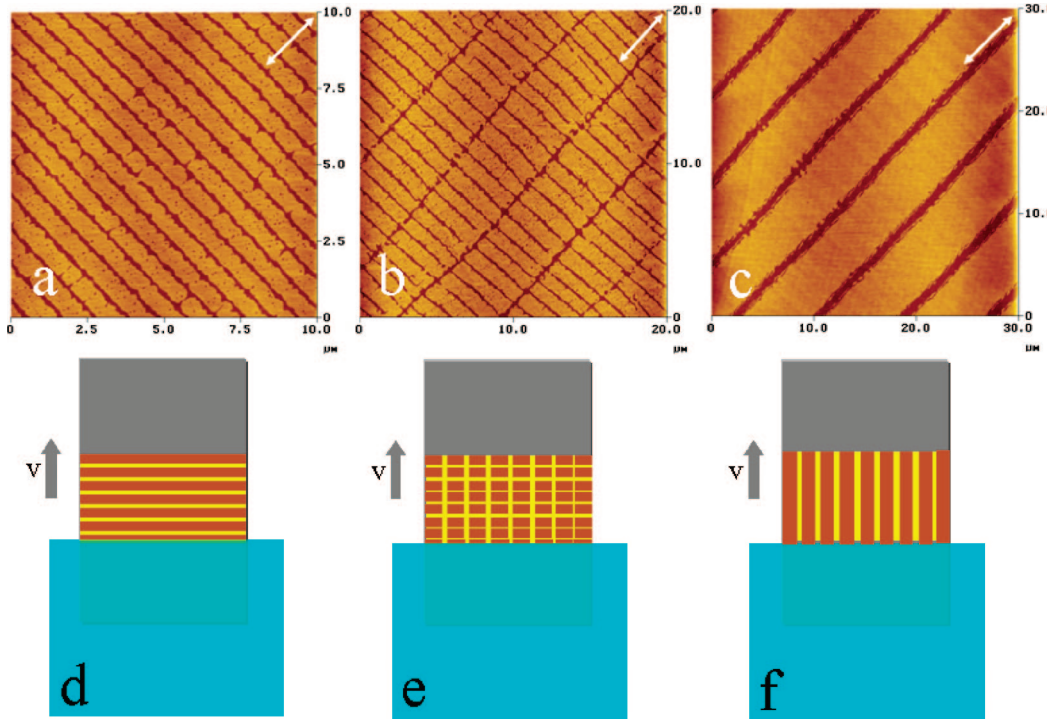

FIGURE 3. Shape and alignment of patterns (pure DPPC) depending upon the transfer conditions. (a–c) AFM images of the various pure DPPC patterns on mica surfaces at (a) 60 mm/min and 3 mN/m, (b) 40 mm/min and 3 mN/m, and (c) 10 mm/min and 3 mN/m. The double arrow in the AFM images shows the axis of film transfer. (d–f) Schematic illustration for the formation of various patterns during the LB vertical deposition.

pressure for forming stripe patterns on RCA-treated (a 5:1:1 mixture of $H_2O/H_2O_2/NH_4OH$ at 70 °C) silicon wafers is higher than for that on oxygen plasma-treated silicon wafers. One possible reason is due to the different interfacial energies of the RCA-treated silicon wafer (106 $\pm$ 3 mJ/m^2) and the oxygen plasma-treated silicon wafer (88 $\pm$ 2 mJ/m^2). Another one is due to the different Si–OH group concentration on the wafer surface, which is an important factor for the substrate-mediated condensation of DPPC molecules during the draining process of water on the substrate.[30] The concentration of Si–OH on the RCA-treated silicon wafer is 34% higher than that on the oxygen plasma-treated silicon wafer. The substrate roughness, which may influence the kinetics of the DPPC phase transition and dynamic contact angle of the meniscus at the three-phase contact line, is likely to be another factor to influence the pattern formation, although this parameter has not yet been systematically studied.

Effect of the Second Component. For a mixed monolayer, the miscibility of various components is important in regard to the phase behavior and the stability of the monolayer. 1,2-Di(2,4-octadecadienoyl)-*sn*-glycero-3-phos-

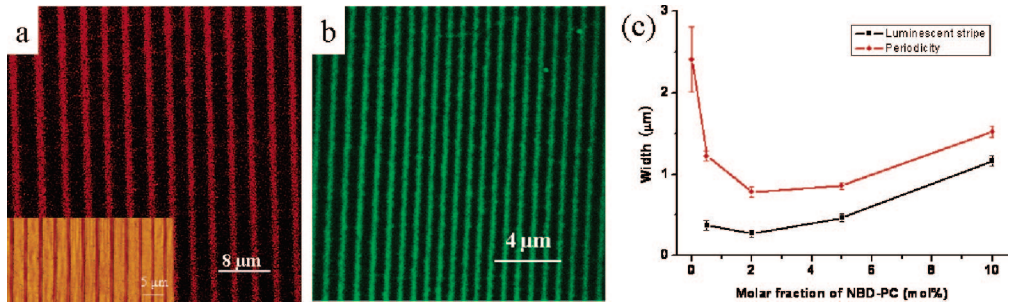

FIGURE 4. (a) Confocal laser scanning microscope (CLSM) image of the regular luminescent stripes formed by DCM/DPPC (5 mol %) at 1.0 mN/m and 10 mm/min (excited at 488 nm and detected at 580–700 nm). The inset in the CLSM image shows an AFM image of the stripe pattern. (b) CLSM images of mixed monolayers of NBD/DPPC (2 mol %) at 2.0 mN/m and 20 mm/min (excited at 488 nm and detected at 500–600 nm). (c) Dependence of the luminescent stripe width and periodicity on the molar fraction of NBD.

phocholine (DOEPC) is selected as an additive component to study the effect of the second component on the DPPC pattern formation during the LB deposition, because DOEPC has a similar molecular structure to DPPC and yet forms a fully LE phase at the air–water interface under the same conditions. In comparison to the pure DPPC monolayer, the pattern formation with the mixed monolayer of DPPC/DOEPC (1:0.1) shifts to lower velocities and higher surface pressures, and the ability to form horizontal stripes is increased.[17] The grid pattern only appears at low transfer velocity (1 mm/min) and high transfer surface pressures. Generally, the size of stripes in the mixed DPPC/DOEPC (1:0.1) patterns is ca. 4–6 times smaller than that of stripes formed by a pure DPPC monolayer at the same transfer conditions.[17]

Other functional molecules, for instance, 4-(dicyanomethylene)-2-methyl-6-(4-dimethylaminostyryl)-4H-pyran (DCM) and 2-(12-(7-nitrobenz-2-oxa-1,3-diazol-4-yl)amino)dodecanoyl-1-hexadecanoyl-*sn*-glycero-3-phosphocholine (NBD), can be used to generate regular and tunable luminescent stripes with submicrometer-scale lateral dimensions (Figure 4).[16] The dye molecules are uniformly distributed within the expanded DPPC channels, which are separated by condensed DPPC stripes. The width and periodicity of the luminescent stripes can be controlled by adjusting the ratio of dye/DPPC, as shown in Figure 4c. It is worth mentioning that some of the dye molecules used [DCM, Nile red, and oligo(*p*-phenylenevinylene)] are nonamphiphilic water-insoluble molecules, suggesting that this method can also be employed for patterning other water-insoluble materials.

Gradient Mesotructured Surface by LB Rotating Transfer. On the basis of the transfer-velocity-dependent pattern formation,[15,17] we further developed a simple yet novel method, LB rotating transfer, to achieve a gradient mesostructure in a well-ordered fashion over large areas.[18] The conventional vertical dipper is only able to move the substrate up or down parallel to the normal of the water surface during the film transfer, and the linear velocity for all points on the whole substrate is constant. During LB rotating transfer, however, the floating monolayer at the air–water interface is transferred onto the substrate

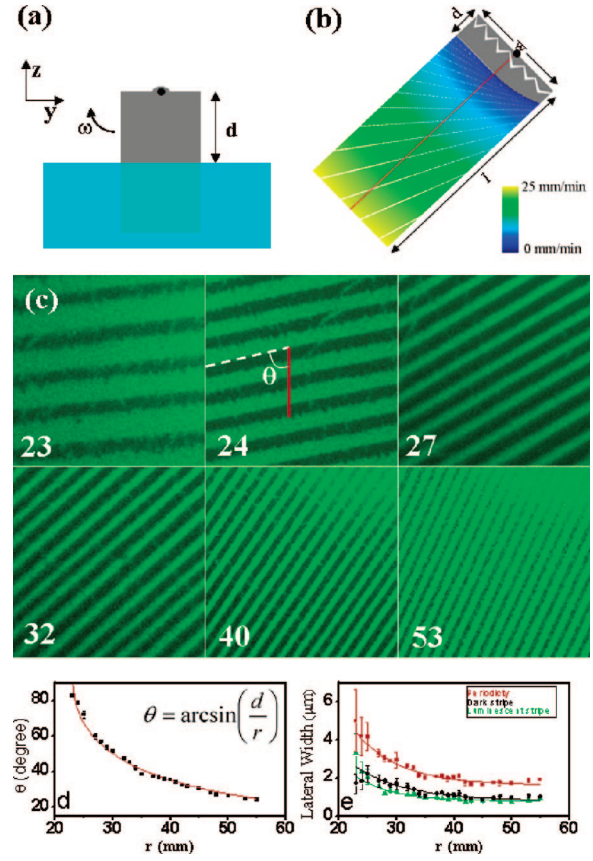

FIGURE 5. (a) Schematic illustration of LB rotating transfer. (b) Simulated distribution of the linear velocity perpendicular to the three-phase contact line (v_v) and orientation (denoted by white lines) of the stripes. $d = 23$ mm, $\omega = 0.07$ rpm, $l = 60$ mm, and $w = 20$ mm. (c) Fluorescence micrographs (30×30 μm^2) of the pattern at various points along the red line in b. The number in each image is the radius (r, mm), and the dotted line is parallel to the three-phase contact line. (d) Dependence of θ on the radius, which could be fitted well (red line, $r^2 = 0.98$) by the theoretical equation. (e) Dependence of the lateral width of the luminescent stripe, dark stripe, and periodicity of gradient patterns on the radius. All data in e are fitted by a mono-exponential decay.

by rotating the substrate along the x axis (Figure 5a), and the linear velocity at different points on the substrate depends upon the distance to the axis of rotation as shown in the simulation results (Figure 5b). As a result, LB patterns with different dimensions and orientations (white

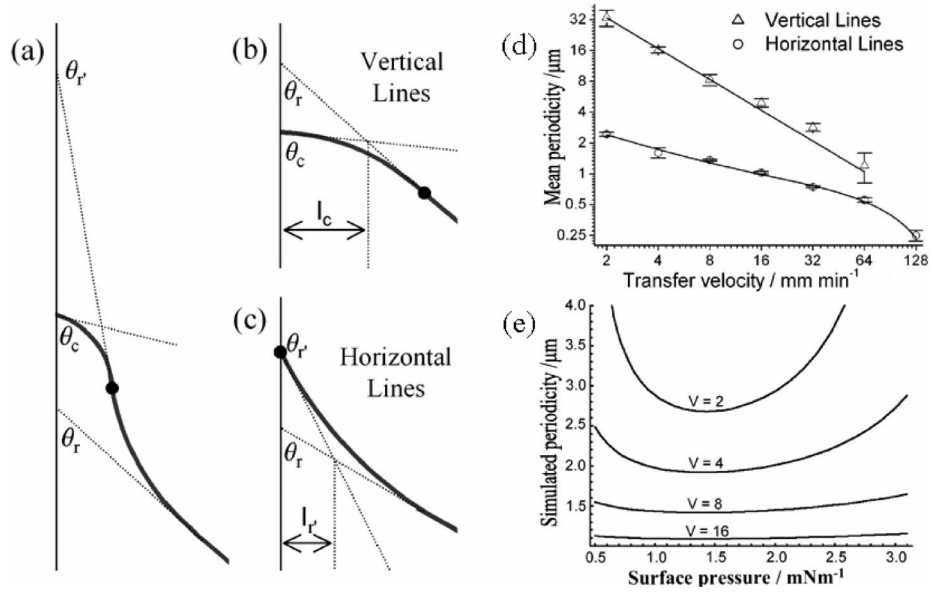

FIGURE 6. (a) Shape of the monolayer-covered air–water interface near the contact line. (b) Region of positive curvature determined by the difference between θ_c and θ_r. (c) Region of negative curvature determined by the difference between θ_r and $\theta_{r'}$. The thicknesses l_c and $l_{r'}$ are defined as the normal distance between the surface and the intersection of the two tangents. (d) Periodicity of the vertical and horizontal lines plotted as a function of transfer velocity. Simulated curves (continuous lines) are fit to the data. (e) Simulated periodicity of the horizontal lines as a function of the surface pressure, shown at different transfer velocities (v, mm/min).

lines in Figure 5b) that depend upon the transfer velocity can be generated simultaneously. Figure 5c shows fluorescence micrographs of gradient stripe patterns along the red line (middle line of the substrate) in Figure 5b, which is formed by the LB rotating transfer of a mixed monolayer of DPPC and NBD (2 mol %) ($\omega = 0.07$ rpm; $\pi = 2$ mN/m). The angle between the red line and the three-phase contact line decreases with an increase in the radius, as shown in Figure 5d, which can fit well to the theoretical expectation. Moreover, the lateral width of the luminescent stripe and the periodicity strongly depend upon the radius: mono-exponentially decreasing with an increasing radii, as shown in Figure 5e. It is easy to extrapolate the ideas presented here to other systems, such as nanoparticles[31,32] and lipid/lipopolymer,[33] to obtain complex arrays and test the experimental conditions for exploring the pattern formation (i.e., high-throughput studies).

Mechanism behind the Pattern Formation. Because the DPPC monolayer is homogeneously in the LE phase of the air–water interface yet consists of heterogeneous condensed and expanded phases after being transferred onto the substrate, substrate-mediated condensation is hypothesized to the origin of the pattern formation.[13,14] During the transfer, a dewetting instability in the vicinity of the three-phase contact line or meniscus oscillation causes a switch of DPPC between the expanded phase (the channels) and the condensed phase (the stripes). One possible mechanism for the switch between these two phases upon transfer is the oscillation of the meniscus height (i.e., stick-slip model), which is correlated to the change in interfacial free energies to satisfy the Young–Laplace condition.[13] This may be true for very slow transfer velocities (0.03–0.24 mm/min), because the oscillation occurs at millihertz frequencies, similar to the nanoparticle systems observed by Yang et al.[32] The second possible explanation is a density oscillation in the vicinity of the three-phase contact line. During the continuous and steady LB transfer, the meniscus shape could be considered as quasi-static[34] and only the region near the three-phase contact line (called the precursor film, which is correlated to the viscous and capillary forces as well as the molecule/substrate interaction) is greatly affected. The kinetic mismatch of the substrate-mediated condensation (on a scale of mm^2/s) and surface molecular diffusion (around 10–100 $\mu m^2/s$) at the precursor film governs the feedback and oscillation of DPPC density, which will lead to the regular pattern formation, and at a higher transfer velocity (>40 mm/min), the frequency of oscillation occurs at kilohertz frequencies. The partitioning of dopants (such as fluorescently labeled lipids) into the expanded channels of the LB pattern suggests that the condensation may be diffusion-limited.[13,16]

The observation that stripes can also form in a different alignment[25] (Figure 3) suggests that the distortion of the shape of the three-phase contact line may govern the switch between transfer modes, and a quantitative model based on the hypothesis that the local curvature near the contact line is behind the switching behavior was therefore developed (Figure 6).[15] The vertical stripes can then be simply explained in terms of a Rayleigh instability: the tendency of a liquid cylinder or rim to break into droplets (△ in Figure 6d). The situation for the horizontal stripes is more complicated, but assuming that condensation is induced by a critical change in the radius of the curvature in the distorted region of the contact line, then the data can be fit by the model (○ in Figure 6d). Finally, simulations indicate that the origin of the regularly spaced striped patterns observed at faster transfer speeds may be due to the lower sensitivity to fluctuations in the local surface density near the three-phase contact line (Figure

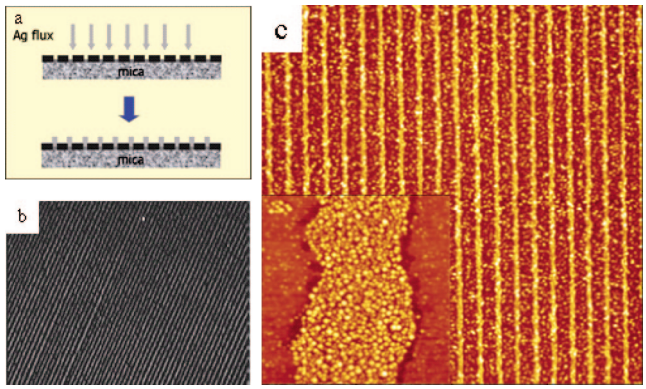

FIGURE 7. (a) Schematic illustration of the process for evaporating silver on a structured surface, and silver atoms deposit preferably onto channel regions. (b) Optical micrograph representing the regular stripe structure over an area of 80 × 60 μm^2. The channels were filled with more silver coating (bright lines), whereas the DPPC stripes appear dark (less silver). (c) AFM image (16 × 16 μm^2) indicates that if a small amount of silver is evaporated (less than 2 nm), then only the channel regions are fully covered, as shown in the inset.

6e). It is worth noting that the present model can only predict the pattern dimensions as a function of experimental parameters. A more rigorous theoretical description of dynamic substrate-mediated condensation that includes the local shape of the meniscus, hydrodynamic effects, interfacial potential energies, molecular interactions, and a nonlinear dynamic model (for instance, a lubrication approximation) quantitatively explaining the meniscus oscillations would likely provide fundamental physical insights into the pattern formation.

Templated Self-Assembly of Molecules and Nanoparticles

As discussed above, the DPPC pattern is composed of expanded DPPC molecules in the channels and condensed DPPC molecules in the stripes. This chemically striped pattern shows anisotropic wetting of 1-phenyloctane, [19] because of the different interfacial energy for the channels (~31 mJ/m^2) and stripes (~23 mJ/m^2).[35] As a result, this kind of mesostructured surface can be used as a template to guide the self-assembly of molecules and nanoparticles.

Templated Self-Assembly of Molecules. The $FeCl_3$ molecules, for instance, condensing from the vapor phase were selectively adsorbed in the channels, whereas the stripes were not coated when a small droplet of $FeCl_3$ solution was brought onto the structured mica surface. Channels filled with paramagnetic $FeCl_3$ molecules provide a contrast in magnetic force microscopy (MFM).[14] In another example, selective adsorption of thermally evaporated silver (2–3 nm) onto the channels was conformed by optical microscopy,[19] as shown in Figure 7. In addition to metals and small molecules that show selective adsorption, Moraille and Badia found that proteins can also selectively adsorb onto the nanostriped surface formed by the mixed monolayer of DPPC and L-α-dilauroylphosphatidylcholine (DLPC).[36] They confirmed that the blood-plasma proteins (human γ globulin and human serum albumin) selectively adsorbed to channels of a nanostructured LB monolayer of

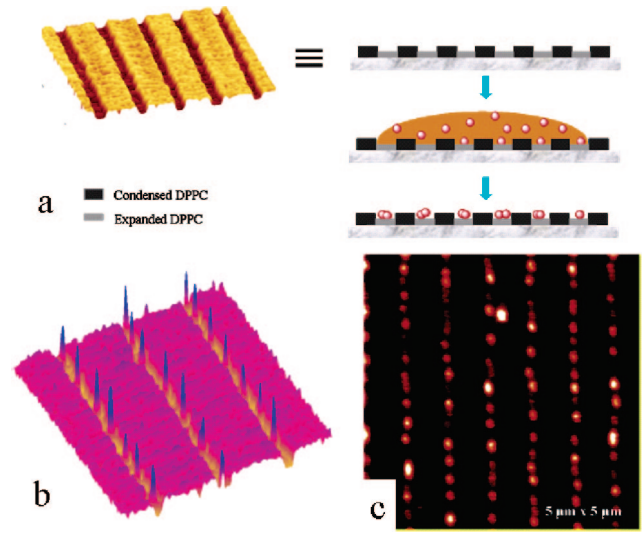

FIGURE 8. (a) Generalized schematic outline of the three steps used to pattern nanoparticles on the DPPC stripe pattern. Selective deposition of (b) Au55 clusters and (c) CdSe nanocrystals aligned along the channels on the mica surface.

DPPC/DLPC to generate well-defined protein and Au nanoparticle/protein patterns.

The DPPC mesostructures on oxygen plasma-treated silicon can be used as templates for directed self-assembly of functional silane molecules to form a robust chemical pattern.[20] A general approach is based on the substitution of the channels and stripes by two different silane molecules (NH_2-terminated and CH_3-terminated silanes) covalently bound to the surface. As a result, a stripe pattern of covalently bound molecules with selective functionality replaced the physisorbed DPPC structure. Then, the negatively charged Au55 clusters can selectively adsorb onto the NH_2-terminated silane stripes because of the electrostatic interaction.[20] Moreover, the NH_2-terminated silane-striped pattern can be used as a template to assist electrodeposition of regular arrays of copper nanowires.[24]

Templated Self-Assembly of Nanoparticles. The DPPC stripe pattern can also serve as a template for selective deposition of nanoparticles simply by dropping the 1-phenyloctane solutions of nanoparticles on the DPPC pattern, as shown in Figure 8. The work of adhesion of 1-phenyloctane on the channels is 62.0 mJ/m^2, which is larger than that of 1-phenyloctane on the stripes (53.7 mJ/m^2). As a result, the nanoparticles accumulate in the expanded DPPC channels when the solution is removed from the sample surface after some time. The density of nanoparticle coverage is determined by the concentration of the nanoparticle solution and the duration of exposure to the patterned surface. As an example, quasi one-dimensional cluster arrays (Figure 8b) of Au55 clusters stabilized by an organic ligand shell were generated.[14] Semiconductor nanocrystals show similar selective adsorption in the channels as well, which was demonstrated by topographical and near-field optical fluorescence measurements (Figure 8c).[21,22] These examples show principally that nanoparticles can be arranged one-dimensionally in a parallel manner over large areas.

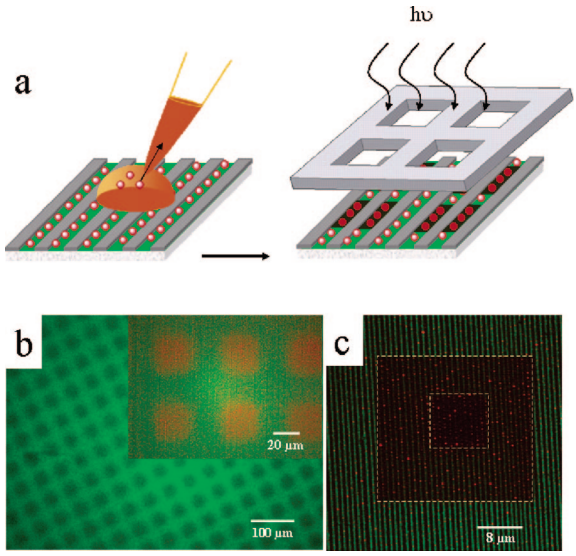

FIGURE 9. (a) Schematic illustration of the procedure for the formation of hierarchical luminescent patterns by exposure to light through a shadow mask. (b) Fluorescence images showing that the photoactivation of CdSe nanocrystals and the photobleaching of BODIPY through a shadow mask reproduced the multiplexed luminescent pattern on the CdSe/BODIPY layer. (c) CLSM image of the multiplex luminescence pattern as a result of different illumination times.

Furthermore, CdSe nanocrystals are also selectively deposited into green-emitting stripes formed by transferring mixed monolayers of DPPC and 2-(4,4-difluoro-5-methyl-4-bora-3a,4a-diaza-*s*-indacene-3-dodecanoyl)-1-hexadecanoyl-*sn*-glycero-3-phosphocholine (BODIPY) (0.5 mol %) onto mica surfaces, for which BODIPY molecules are uniformly distributed within the expanded DPPC channels.[23] On the basis of the photoinduced enhancement of the fluorescence of CdSe nanocrystals[37] and photobleaching of dyes, a hierarchical luminescence pattern is generated, as shown in Figure 9. Figure 9b shows the hierarchical luminescence pattern that was obtained by exposing the samples to light through a shadow mask (500 mesh copper grid, square holes with sides of 28 μm). The areas exposed to the light (the squares) appear red, and the green lines correspond to the regions shielded by the mask. Furthermore, we produced another kind of hierarchical luminescence pattern, as shown in Figure 9c, in which the different squares are exposed to light for different amounts of time according to the time dependence of the photobleaching of BODIPY and fluorescence enhancement of CdSe nanocrystals. The exposure time for the inside square is longer than the exposure time for the outside square; therefore, we only observe red dot arrays in the inside square, while orange dots are present on the green stripes in the outside square.

Pattern Transfer—From Chemical to Topographical Patterns

LB Lithography. The self-organized DPPC LB patterns as well as other LB patterns, such as chiral domains,[12,25] can be used as resistance against wet chemical etching by using a very dilute alkaline etchant (e.g., KOH) and long

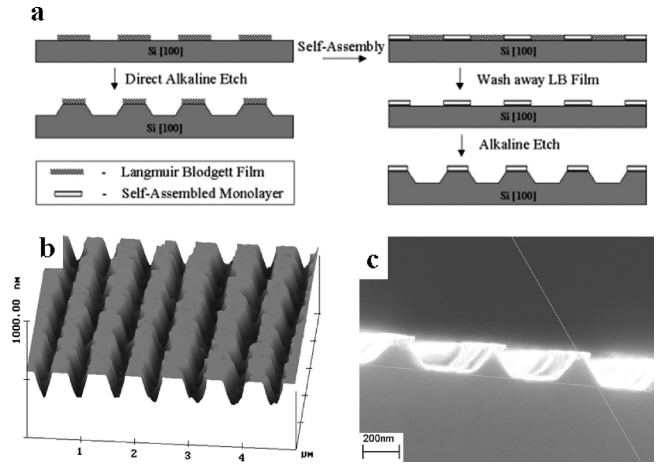

FIGURE 10. (a) Schematic illustration of the chemical-etch process used to transfer LB patterns into topographical features. Groove depth and local periodicity were characterized by (b) AFM and (c) scanning electron microscopy.

etch time (~12 h), termed LB lithography.[25] This allows the patterns to be converted into topographical features in silicon (Figure 10). An etch selectivity >100 (etch depth/resist thickness) is achieved, and the depth of the etching can be controlled between 20 and 300 nm by variation in the etch time.

Nanotopography-Directed Growth of Biological Cells. The topographically patterned silicon obtained by LB lithography can be used as masters to generate replicas by means of nanoimprinting and replica molding. This is interesting for certain applications such as the culturing of biological cells, where it is desirable to be able to mass produce a large number of identical surfaces. We demonstrated this possibility by using the nanostructured silicon surfaces as masters for hot embossing of polystyrene,[25,26] as shown in Figure 11a. For the first step, the silicon master is placed in contact with the polymer under slight pressure and the system is heated above the glass transition temperature of the polymer. The polymer is then cooled below the transition temperature and peeled from the master. After this, the master can be reused to serially produce hundreds of replicas without a noticeable decrease in the quality.

Square centimeter surface areas of polystyrene topographically patterned by submicrometer-scale grooves were used to study the influence of surface textures on primary osteoblast cell morphology, mobility, and even differentiation.[25,26] Cells cultured for 24 h on grooved polystyrene surfaces with a periodicity of 500 nm were observed to align with the grooves, as shown in parts b and c of Figure 11. Moreover, the osteoblasts showed a stronger alignment on deeper grooves, while the number of cells attaching to the structured surfaces with different depths (50 and 150 nm, as well as on a smooth control) appeared to be unaffected by the nanotopography of the surface. Immunohistochemical staining of aligned cells indicated the presence of focal adhesions at opposite ends of aligned cells. A significant anisotropic migration was observed on both the 50 and 150 nm deep grooves, again to a larger extent on the deeper grooves.[26] In addition to

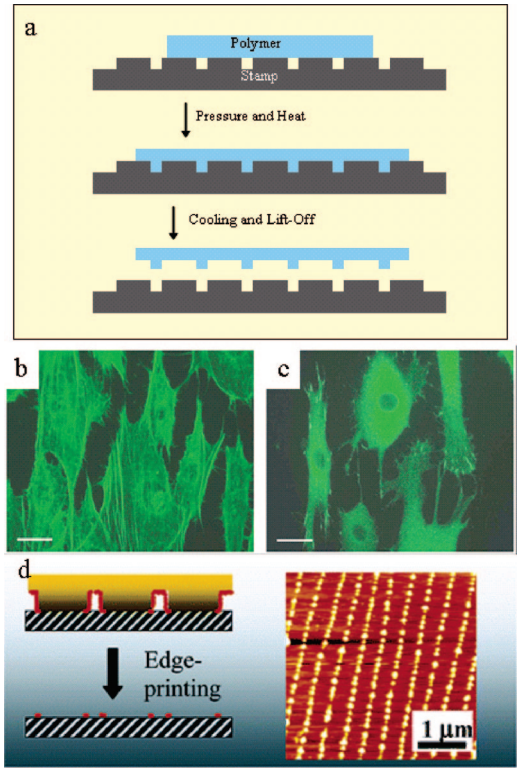

FIGURE 11. (a) Schematic process for pattern transfer from a silicon master to polystyrene. Fluorescence micrographs of osteoblasts aligned on 150 nm deep grooves, labeled for (b) actin and (c) vinculin. Bar = 20 μm. (d) Edge printing of semiconductor nanocrystals by the interfacial interaction-controlled transport of CdTe nanocrystals.

osteoblasts, other types of cells including the phytopathegenic fungi *Magnaporthe grisea* and *Pucinnia graminis* also align on the groved patterns fabricated by LB lithography (to be published). The ability to economically mass produce large surface areas patterned with different nanotopography opens new possibilities, both in the scientific understanding of the mechanisms behind contact guidance and in the optimization of surfaces for biological applications.

Microcontact Printing of Semiconductor Nanocrystals. The structured polystyrene surfaces can be further used as masters for replica molding of polydimethoxysiloxane (PDMS).[27] This is done by pouring the PDMS precursors over the polystyrene topographies and curing at 60 °C (well below the glass-transition temperature of polystyrene) for 2 h. The PDMS stamp can then be readily peeled from the polystyrene master. The advantage of this two-step process is that the PDMS replica molding can then be carried out in parallel, allowing for the simple and rapid fabrication of numerous low-cost identical copies. This structured PDMS can then be used for microcontact printing, for instance, to pattern CdTe nanocrystals on SiO_2/Si surfaces (Figure 11d).[27] Either edge or homogeneous printing can be achieved under optimized conditions.

Conclusion and Outlook

In summary, we described our recent works on the fabrication of well-ordered mesoscopic structural surfaces over large areas by the LB technique, which is contrary to the historic research of LB films, which focused on obtaining uniform and defect-free films.[8] The results presented in this Account show that dynamic self-organization and template-directed self-assembly may be able to successfully control and modify the surface patterning, which is a prerequisite if LB patterning is to become a candidate for the assembly of nanostructures into integrated device architectures.[38–41] Similar LB patterning has been recently reported in fatty acid methyl and ethyl esters,[42] nanoparticles,[31,32] and lipid/lipopolymer-mixed monolayer systems,[33] opening the possibility of extending this method to other pattern-generating chemical systems. The mesoscopic structural surfaces described here may serve as a platform in engineering the biological/material interface, for instance, surfaces for controlled cell adhesion and specific interactions with biocomponents. Moreover, in combination with biomaterials (protein, DNA, and polysaccharide), mesoscopically structured surfaces may contribute to the construction of biofunctionalized structures and "programmed" systems.

We thank former group members, especially M. Gleiche, M. Zhang, and X. Wu, for contributing to the work summarized herein. We acknowledge the fruitful collaboration with G. Schmid, A. L. Rogach, M. Wang, and L. Wu. This work is supported by GIF and SFB 424.

References

(1) Ball, P. *The Self-Made Tapestry: Pattern Formation in Nature*; Oxford University Press: Oxford, U.K., 1999.
(2) Menz, W.; Mohr, J.; Paul, O. *Microsystem Technology*, 2nd ed.; Wiley-VCH: Weinheim, Germany, 2001.
(3) Rosi, N. L.; Mirkin, C. A. Nanostructures in Biodiagnostics. *Chem. Rev.* **2005**, *105*, 1547–1562.
(4) Gates, B. D.; Xu, Q. B.; Stewart, M.; Ryan, D.; Willson, C. G.; Whitesides, G. M. New Approaches to Nanofabrication: Molding, Printing, and Other Techniques. *Chem. Rev.* **2005**, *105*, 1171–1196.
(5) Ito, T.; Okazaki, S. Pushing the Limits of Lithography. *Nature* **2000**, *406*, 1027–1031.
(6) Geissler, M.; Xia, Y. N. Patterning: Principles and Some New Developments. *Adv. Mater.* **2004**, *16*, 1249–1269.
(7) Gains, L. G. *Insoluble Monolayers at Liquid–Gas Interfaces*; Interscience Publishers: New York, 1969.
(8) Roberts, G. *Langmuir–Blodgett Films*; Plenum Press: New York, 1990.
(9) Chen, X. D.; Wang, J. B.; Shen, N.; Luo, Y. H.; Li, L.; Liu, M. H.; Thomas, R. K. Gemini Surfactant/DNA Complex Monolayers at the Air–Water Interface: Effect of Surfactant Structure on the Assembly, Stability, and Topography of Monolayers. *Langmuir* **2002**, *18*, 6222–6228.
(10) Huang, X.; Li, C.; Jiang, S. G.; Wang, X. S.; Zhang, B. W.; Liu, M. H. Self-Assembled Spiral Nanoarchitecture and Supramolecular Chirality in Langmuir–Blodgett Films of an Achiral Amphiphilic Barbituric Acid. *J. Am. Chem. Soc.* **2004**, *126*, 1322–1323.
(11) Chen, X. D.; Wang, J. B.; Liu, M. H. Influence of Surfactant Molecular Structure on Two-Dimensional Surfactant–DNA Complexes: Langmuir Balance Study. *J. Colloid Interface Sci.* **2005**, *287*, 185–190.
(12) Zhang, L.; Gaponik, N.; Muller, J.; Plate, U.; Weller, H.; Erker, G.; Fuchs, H.; Rogach, A. L.; Chi, L. F. Branched Wires of CdTe Nanocrystals Using Amphiphilic Molecules as Templates. *Small* **2005**, *1*, 524–527.
(13) Spratte, K.; Chi, L. F.; Riegler, H. Physisorption Instabilities during Dynamic Langmuir Wetting. *Europhys. Lett.* **1994**, *25*, 211–217.
(14) Gleiche, M.; Chi, L. F.; Fuchs, H. Nanoscopic Channel Lattices with Controlled Anisotropic Wetting. *Nature* **2000**, *403*, 173–175.

(15) Lenhert, S.; Gleiche, M.; Fuchs, H.; Chi, L. F. Mechanism of Regular Pattern Formation in Reactive Dewetting. *ChemPhysChem* **2005**, *6*, 2495–2498.
(16) Chen, X. D.; Hirtz, M.; Fuchs, H.; Chi, L. F. Self-Organized Patterning: Regular and Spatially Tunable Luminescent Submicrometer Stripes over Large Areas. *Adv. Mater.* **2005**, *17*, 2881–2885.
(17) Chen, X. D.; Lu, N.; Zhang, H.; Hirtz, M.; Wu, L. X.; Fuchs, H.; Chi, L. F. Langmuir–Blodgett Patterning of Phospholipid Microstripes: Effect of the Second Component. *J. Phys. Chem. B* **2006**, *110*, 8039–8046.
(18) Chen, X. D.; Hirtz, M.; Fuchs, H.; Chi, L. F. Fabrication of Gradient Mesostructures by Langmuir–Blodgett Rotating Transfer. *Langmuir* **2007**, *23*, 2280–2283.
(19) Gleiche, M.; Chi, L. F.; Gedig, E.; Fuchs, H. Anisotropic Contact-Angle Hysteresis of Chemically Nanostructured Surfaces. *ChemPhysChem* **2001**, *2*, 187–191.
(20) Lu, N.; Gleiche, M.; Zheng, J. W.; Lenhert, S.; Xu, B.; Chi, L. F.; Fuchs, H. Fabrication of Chemically Patterned Surfaces Based on Template-Directed Self-Assembly. *Adv. Mater.* **2002**, *14*, 1812–1815.
(21) Lu, N.; Chen, X. D.; Molenda, D.; Naber, A.; Fuchs, H.; Talapin, D. V.; Weller, H.; Muller, J.; Lupton, J. M.; Feldmann, J.; Rogach, A. L.; Chi, L. F. Lateral Patterning of Luminescent CdSe Nanocrystals by Selective Dewetting from Self-Assembled Organic Templates. *Nano Lett.* **2004**, *4*, 885–888.
(22) Naber, A.; Molenda, D.; Fischer, U. C.; Maas, H. J.; Hoppener, C.; Lu, N.; Fuchs, H. Enhanced Light Confinement in a Near-Field Optical Probe with a Triangular Aperture. *Phys. Rev. Lett.* **2002**, *89*, 210801.
(23) Chen, X. D.; Rogach, A. L.; Talapin, D. V.; Fuchs, H.; Chi, L. F. Hierarchical Luminescence Patterning Based on Multiscaled Self-Assembly. *J. Am. Chem. Soc.* **2006**, *128*, 9592–9593.
(24) Zhang, M. Z.; Lenhert, S.; Wang, M.; Chi, L. F.; Lu, N.; Fuchs, H.; Ming, N. B. Regular Arrays of Copper Wires Formed by Template-Assisted Electrodeposition. *Adv. Mater.* **2004**, *16*, 409–413.
(25) Lenhert, S.; Zhang, L.; Mueller, J.; Wiesmann, H. P.; Erker, G.; Fuchs, H.; Chi, L. F. Self-Organized Complex Patterning: Langmuir–Blodgett Lithography. *Adv. Mater.* **2004**, *16*, 619–624.
(26) Lenhert, S.; Meier, M. B.; Meyer, U.; Chi, L. F.; Wiesmann, H. P. Osteoblast Alignment, Elongation and Migration on Grooved Polystyrene Surfaces Patterned by Langmuir–Blodgett Lithography. *Biomaterials* **2005**, *26*, 563–570.
(27) Wu, X. C.; Lenhert, S.; Chi, L. F.; Fuchs, H. Interface Interaction Controlled Transport of CdTe Nanoparticles in the Microcontact Printing Process. *Langmuir* **2006**, *22*, 7807–7811.
(28) McConnell, H. M. Structures and Transitions in Lipid Monolayers at the Air–Water Interface. *Ann. Rev. Phys. Chem.* **1991**, *42*, 171–195.
(29) Mohwald, H. Phospholipid and Phospholipid–Protein Monolayers at the Air/Water Interface. *Ann. Rev. Phys. Chem.* **1990**, *41*, 441–476.
(30) Petrov, J. G.; Radoev, B. P. Steady Motion of the 3 Phase Contact Line in Model Langmuir–Blodgett Systems. *Colloid Polym. Sci.* **1981**, *259*, 753–760.
(31) Huang, J. X.; Kim, F.; Tao, A. R.; Connor, S.; Yang, P. D. Spontaneous Formation of Nanoparticle Stripe Patterns through Dewetting. *Nat. Mater.* **2005**, *4*, 896–900.
(32) Huang, J. X.; Tao, A. R.; Connor, S.; He, R. R.; Yang, P. D. A General Method for Assembling Single Colloidal Particle Lines. *Nano Lett.* **2006**, *6*, 524–529.
(33) Purrucker, O.; Fortig, A.; Ludtke, K.; Jordan, R.; Tanaka, M. Confinement of Transmembrane Cell Receptors in Tunable Stripe Micropatterns. *J. Am. Chem. Soc.* **2005**, *127*, 1258–1264.
(34) Petrov, P. G.; Petrov, J. G. Extrapolated Dynamic Contact-Angle and Viscous Deformation of a Steady Moving Meniscus at a Vertical Flat Wall. *Langmuir* **1995**, *11*, 3261–3268.
(35) Berger, C. E. H.; Vanderwerf, K. O.; Kooyman, R. P. H.; Degrooth, B. G.; Greve, J. Functional-Group Imaging by Adhesion AFM Applied to Lipid Monolayers. *Langmuir* **1995**, *11*, 4188–4192.
(36) Moraille, P.; Badia, A. Spatially Directed Protein Adsorption by Using a Novel, Nanoscale Surface Template. *Angew. Chem., Int. Ed.* **2002**, *41*, 4303–4306.
(37) Wang, Y.; Tang, Z. Y.; Correa-Duarte, M. A.; Pastoriza-Santos, I.; Giersig, M.; Kotov, N. A.; Liz-Marzan, L. M. Mechanism of Strong Luminescence Photoactivation of Citrate-Stabilized Water-Soluble Nanoparticles with CdSe Cores. *J. Phys. Chem. B* **2004**, *108*, 15461–15469.
(38) Lu, N.; Zheng, J. W.; Gleiche, M.; Fuchs, H.; Chi, L. F.; Vidoni, O.; Reuter, T.; Schmid, G. Connecting Nanowires Consisting of Au-55 with Model Electrodes. *Nano Lett.* **2002**, *2*, 1097–1099.
(39) Whang, D.; Jin, S.; Wu, Y.; Lieber, C. M. Large-Scale Hierarchical Organization of Nanowire Arrays for Integrated Nanosystems. *Nano Lett.* **2003**, *3*, 1255–1259.
(40) Whang, D.; Jin, S.; Lieber, C. M. Nanolithography Using Hierarchically Assembled Nanowire Masks. *Nano Lett.* **2003**, *3*, 951–954.
(41) Jin, S.; Whang, D. M.; McAlpine, M. C.; Friedman, R. S.; Wu, Y.; Lieber, C. M. Scalable Interconnection and Integration of Nanowire Devices without Registration. *Nano Lett.* **2004**, *4*, 915–919.
(42) Chi, L. F.; Jacobi, S.; Anczykowski, B.; Overs, M.; Schafer, H. J.; Fuchs, H. Supermolecular Periodic Structures in Monolayers. *Adv. Mater.* **2000**, *12*, 25–30.

AR600019R